Fungal Biology 130 (2026) 101775

Contents lists available at ScienceDirect

Fungal Biology

journal homepage: www.elsevier.com/locate/funbio

Cytoplasmic flow dynamics in arbuscular mycorrhizal fungi are intrinsic and independent of plant hosts

Malin Klein [a,b,c,*], Loreto Oyarte Gálvez [a,c], Daniel van der Lugt [a], Corentin Bisot [a,c,d], Simon van Staalduine [c], Stuart A. West [e], Vasilis Kokkoris [f], Lemeng Dong [b], Harro Bouwmeester [b], Thomas S. Shimizu [c], James T. Weedon [f], E. Toby Kiers [a,g]

[a] Section Ecology and Evolution, Amsterdam Institute for Life and Environment, Vrije Universiteit Amsterdam, Amsterdam, Netherlands
[b] Plant Hormone Biology, Swammerdam Institute for Life Sciences, University of Amsterdam, Amsterdam, Netherlands
[c] Physics of Behavior, AMOLF Institute, Amsterdam, Netherlands
[d] Laboratoire Reproduction et Développement des Plantes, Univ Lyon, ENS de Lyon, UCB Lyon 1, CNRS, INRAE, INRIA, Lyon, France
[e] Department of Biology, Oxford University, United Kingdom
[f] Section Systems Ecology, Amsterdam Institute for Life and Environment, Vrije Universiteit Amsterdam, Amsterdam, Netherlands
[g] Society for the Protection of Underground Networks (SPUN), Dover, DE, USA

ARTICLE INFO

Keywords:
Arbuscular mycorrhizal fungi
Myristic acid
Cytoplasm flows
Spores
Symbiosis
Evolution

ABSTRACT

Despite the ecological importance of arbuscular mycorrhizal (AM) fungi, it is unclear to what extent these symbionts can act autonomously from plant hosts, especially in their ability to control internal nutrient flows. We studied flows in AM fungal networks grown without plant hosts by providing myristic acid as a carbon source.

Using a custom-built imaging platform, we tracked network formation of two *Rhizophagus irregularis* strains with and without myristic acid. We collected 5000 cytoplasmic flow videos in hyphae, and fluorescently tagged lipids to measure their speeds. We measured ~25,000 flow trajectories and calculated flow speeds by kymograph analysis.

In the presence of myristic acid but lacking a host root, AM fungi produced networks 10-times longer, covered up to 4 times more area, and showed a 50% increase in mean flow speed. Flow speeds varied drastically over time and space, with rare bursts of fast flows between 10 and 30 μm/s. Flows of fluorescently tagged lipids averaged 3 μm/s and were unaffected by myristic acid. Even one year after application, we could detect cytoplasmic flows in asymbiotic fungal hyphae close to parental spores when grown with myristic acid.

Our findings suggest that cytoplasmic flows can be decoupled from hosts and challenge our current understanding of AM fungal autonomy.

1. Introduction

Arbuscular mycorrhizal (AM) fungi are important and ubiquitous symbionts of ~70% of all plant species, found across most of Earth's terrestrial ecosystems (Brundrett and Tedersoo, 2018). These AM fungi form underground hyphal networks that colonize the roots of their host plants. AM fungi draw down an estimated 4 Gt CO_2 into soils every year (Hawkins et al., 2023) and provide many other important functions, including nutrient uptake and water acquisition (Kakouridis et al., 2022; Stock et al., 2021;Kuyper et al., 2021), soil aggregation (Gómez-Leyva et al., 2023;Řezáčová et al., 2021), and plant health benefits (Gashgari et al., 2020;Tang et al., 2023).

The AM fungal symbiosis relies on nutrient exchange partnerships: fungi provide nutrients such as phosphorus (P) and nitrogen (N) and receive carbon from the plant which they use to grow their networks (Kuyper et al., 2021;Stock et al., 2021). AM fungi are considered obligate biotrophs because they lack intrinsic fatty acid synthesis (Trépanier et al., 2005;Wewer et al., 2014) and depend on host roots for carbon, specifically sugars and lipids (Bago et al., 2000;Jiang et al., 2017; Luginbuehl et al., 2017;Schubert et al., 2003). AM fungi can actively move nutrients through their open-pipe (aseptate) hyphal networks, so that they can rapidly move nutrients to plants and carbon to their own fungal tips (Cargill et al., 2025). Cytoplasmic flow velocities in pre-symbiotic germlings have been subject to investigation for decades

* Corresponding author. Section Ecology and Evolution, Amsterdam Institute for Life and Environment, Vrije Universiteit Amsterdam, Amsterdam, Netherlands.
E-mail address: m.klein@vu.nl (M. Klein).

https://doi.org/10.1016/j.funbio.2026.101775
Received 15 January 2026; Received in revised form 6 May 2026; Accepted 11 May 2026
Available online 13 May 2026

(Giovannetti et al., 1999, 2000). Recent quantitative research has confirmed that within the thin hyphae of symbiotic network, cytoplasm can stream in two directions simultaneously (Oyarte Galvez et al., 2025). The bidirectionality is necessary because the carbon in the hyphae must be transported long range from the host root toward the hyphal tips. This allows the network to build a colonization front in search of new roots and nutrients. Simultaneously, nutrients such as P and N foraged from the soil, are moved through the fungal network toward the host root (Oyarte Galvez et al., 2025).

Previous research has focused on how hosts influence the nutrient exchange patterns of AM fungi. For example, the resource transfer from a fungus to the host is highly variable and can depend on factors including host species (Torrecillas et al., 2012;Šmilauer et al., 2019), host light availability (Knegt et al., 2016), host root architecture and even host age (Šmilauer et al., 2021). However, it is unclear to what extent AM fungi can act autonomously from their host plants, especially regarding the degree to which they control the speed and direction of their nutrient flows. There are two contrasting hypotheses concerning fungal autonomy, which represent extreme ends of a possible continuum. First, since in AM fungal carbon comes exclusively from plants, host roots could play a major role in regulating hyphal flow dynamics. This possibility is supported by the observation that flows in AM fungi are positively correlated to the host plant's transpiration (Kikuchi et al., 2016). An alternative possibility is that although the host may control the exact amount of carbon, it is the fungus that controls the regulation of flows. Past work has explored flows generated in fungal networks (Hammer et al., 2024; Whiteside et al., 2019), but whether attachment to the host is required for those flow dynamics remains unknown. An ideal experiment to resolve these hypotheses would decouple the plant-fungal symbiosis so that nutrient flows within AM fungal networks can be quantified in the absence of a plant host.

We addressed this challenge by using a recently discovered method (Sugiura et al., 2020) for growing AM fungi without a host by providing myristic acid as a fatty acid carbon source. Intracellularly, myristic acid is involved in lipid modification of proteins such as N-myristoylation for membrane anchoring (Sonnenburg and Gordon, 2013) and can provide energy through ATP generation by oxidation (Kohlmeier, 2015). Myristic acid has also been reported as a compound in plant root exudates (S. Li et al., 2017; Pomilio et al., 2000; Xing et al., 2024) and as a bacterial product (Hildebrandt et al., 2006; M. Saito et al., 2018). Past *in vitro* and greenhouse work has shown that exogenous myristic acid and its salts increase root colonization by AM fungi (Chen et al., 2025; Liu et al., 2023; Xing et al., 2024). Myristic acid allows AM fungi to grow asymbiotically and produce infective daughter spores by providing energy in form of ATP and carbon (Sugiura et al., 2020; Tanaka et al., 2022). Our aim was to quantify cytoplasmic spatiotemporal flow behavior inside AM fungal asymbiotic networks by using myristic acid as an external carbon and energy source (Sugiura et al., 2020). We did this by germinating spore clusters of two *Rhizophagus irregularis* strains in the presence and absence of exogenous myristic acid.

We first tracked the hyphal growth across replicates using a custom-built imaging robot (Oyarte Galvez et al., 2025). We identified specific regions of interest across the network topology of developing hyphae (e.g., near parent spores, far from and near hyphal branching points, and next to hyphal tips) and used brightfield microscopy to record cytoplasmic flows over a period of six weeks. To test how carbon moves through non-symbiotic networks, we labeled neutral lipids with a carbon-specific florescent tag and recorded lipid dynamics using fluorescence microscopy. We extracted flow velocities using kymograph analysis (Mangeol et al., 2016). To examine longevity of asymbiotic networks, we recorded these measurements in selected plates after one year of asymbiotic growth.

Using these datasets, we asked the following questions (Q1) Is the bidirectionality of cytoplasmic flows conserved in the absence of a host and (Q2) how does the exogenous carbon source affect the flow speed of the cytoplasm, including lipids specifically (Q3) Does the application of myristic acid as external carbon source positively affect the growth and flows of different AM fungi strains equally?

2. Materials and methods

2.1. Media

We used MSR medium with 0.3% (w/v) Phytagel™ with and without 0.5 mM myristic acid as a substrate for AM fungal network growth as described in the Supplemental Methods.

2.2. Fungal material

We used spore clusters of *R. irregularis* strains A5 (DAOM 664344) and C2 (DAOM 664346) that we isolated as described in the Supplemental Methods. We placed the clusters in the center of each plate (Suppl. Table 1). All plates were sealed with parafilm and incubated lid facing upwards in the dark at 25 °C.

To track carbon flows in the cytoplasmic streams, we stained a subset of plates of each strain and treatment with Nile red as described in the Supplemental Methods. After overnight incubation at 25 °C in the dark, we recorded videos in brightfield first, followed by imaging in the fluorescence channel.

2.3. Image acquisition and data extraction

2.3.1. Network growth experiment

We imaged all plates for 2 months (57 days) every 2-4 h on a customized platform in an enclosed, dark, and temperature-controlled environment described in detail in (Oyarte Galvez et al., 2025) and in brief in the Supplemental Methods. We obtained network total hyphal length (mm) and network area (mm^2) following the method described in (Oyarte Galvez et al., 2025). To account for differences in numbers of spores between plates, we standardized network length and area by the number of parent spores. We calculated network density (mm/mm^2) by dividing network length by area. We manually counted newly formed spores in the region approximately 10 × 10 mm around the parent spores using the multi-point tool in FIJI – ImageJ v. 2.1.0/1.53c (Schindelin et al., 2012) (Suppl. Fig. 2, Suppl. Table 2).

2.3.2. Cytoplasmic flow experiment

For an overview of the location and number of initial spores on our customized platform, we imaged all plates at the start of the experiment. At each recording date (days within weeks 2, 3, 4, 5, and 6), we created a map of the network image, extracted architecture characteristics, and identified regions of interest for video imaging (e.g., near parent spores, far from and near hyphal branching points, and next to hyphal tips). We recorded videos of cytoplasmic streaming on a second customized platform described in (Oyarte Galvez et al., 2025) and in the Supplemental Methods. We generated and selected kymographs and extracted the cytoplasm flow speeds as described in the Supplemental Methods and shown Supplemental Fig. 1.

We determined the distance of each video location from the location of the parent spores in a straight line by using the recorded coordinates of each video (Suppl. Fig. 2a). Videos with missing coordinates due to recording malfunction were excluded from this part of the analysis.

2.4. Statistical analyses

We analyzed the data using GLM and linear-mixed-effects models as described in detail in the Supplemental Methods and Supplemental Table 3. All statistical analyses were performed using R statistical software (v4.2.2) (R Core Team, 2022) with the packages lme4 (version 1.1-37) for linear mixed-effects models (Bates et al., 2015) and emmeans (version 1.8.4-1) for contrasts (Lenth et al., 2023).

3. Results

3.1. Effect of external carbon source myristic acid on asymbiotic network growth and spore production

By measuring length and area of the networks every 2-4 h for 2 months, we could quantify how asymbiotic AM fungal networks developed with and without the addition of myristic acid (Fig. 1). We found that the addition of myristic acid as an external carbon and energy source led to hyphal networks that were larger, denser, and produced more spores.

We observed that myristic acid addition had a significant effect on maximum network length ($F = 142.3$, $p < 0.001$) with this positive effect not significantly differing between the two strains (interaction $F = 0.2$, $p = 0.66$). In the absence of myristic acid (control, 0 mM myristic acid), there was very little growth in both A5 and C2 strains. In comparison, networks demonstrated substantial growth when 0.5 mM myristic acid was added as external carbon source (Fig. 2A). Similarly, myristic acid had a significant effect on the network area ($F = 86.1$, $p < 0.001$) but this positive effect did not differ between the two strains (interaction $F = 1.6$, $p = 0.23$). Density (mm/mm^2) was also significantly affected by treatment ($F = 20.4$, $p = 0.0006$) and this positive effect did not differ between the two strains (interaction $F = 2.1$, $p = 0.18$). We found that strain and treatment, but not their interaction, had a significant effect on the number of newly produced spores (strain: $F = 23.33$, $p = 0.0002$, treatment: $F = 58.58$, $p < 0.0001$, strain:treatment: $F = 3.94$, $p = 0.07$).

In terms of total length, we found A5 and C2 grew 10-fold longer hyphae in myristic acid conditions than in control conditions (Fig. 2A). Germinating C2 spores produced longer networks in myristic acid conditions (mean ± standard deviation, 1276 ± 548 mm) than in control conditions (98.9 ± 47.1 mm, $p < 0.0001$). Likewise, the network length of germinating A5 spores in myristic acid conditions (865 ± 381 mm) was significantly larger than in the controls (50.4 ± 14.7 mm,

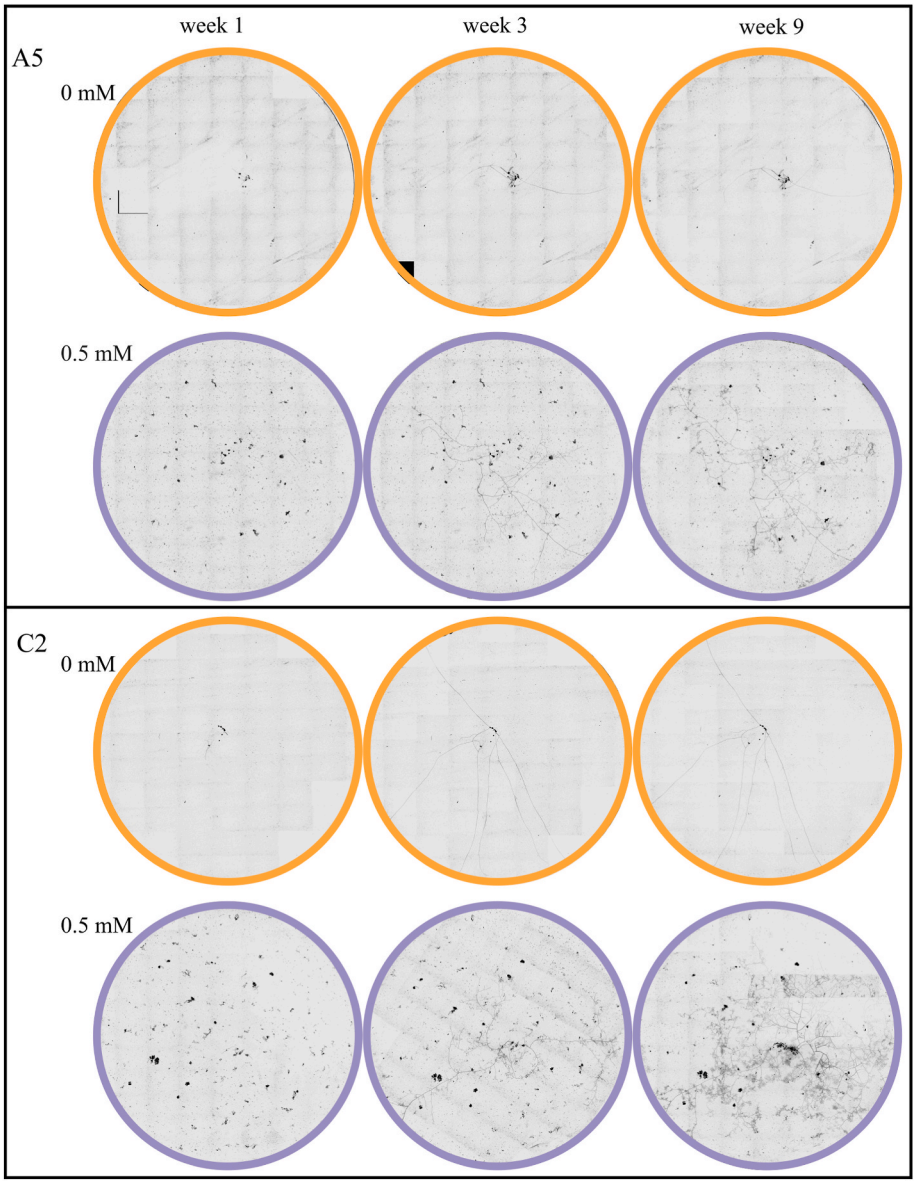

Fig. 1. Hyphal growth over time of *R. irregularis* strains A5 and C2 in the presence (0.5 mM, purple) and absence (0 mM, orange) external myristic acid at the start of the experiment (week 1) and then two and eight weeks later of four example replicates. In control conditions (0 mM myristic acid, orange), both strains germinate and grow hyphae. When myristic acid is present as exogenous carbon source (0.5 mM, purple), both strains germinate and grow more complex networks. In week 9, myristic acid crystals (dark spots in the media with 0.5 mM myristic acid; absent in the control conditions) are still visible by eye. (For interpretation of the references to color in this figure legend, the reader is referred to the Web version of this article.)

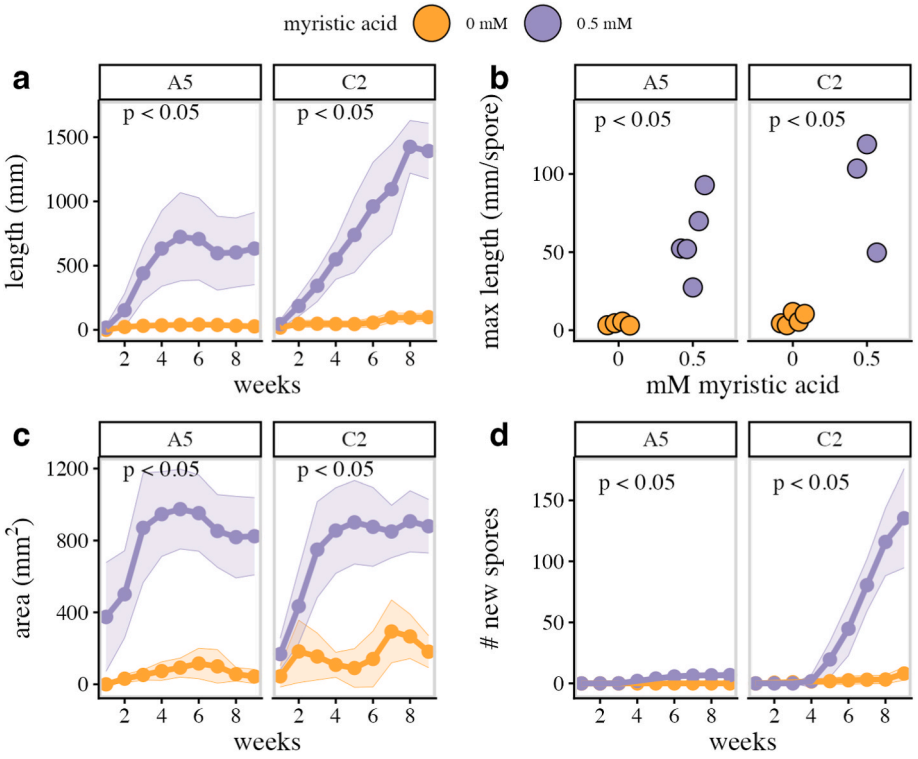

Fig. 2. Network and spore development of *R. irregularis* strains A5 and C2 in control (orange) and 0.5 mM myristic acid (purple) conditions. **A)** Development of hyphal length of strains A5 and C2 over 9 weeks. The shaded region indicates the range of standard deviation. Significance level $p < 0.05$ determined by Tukey test. **B)** Final length of hyphae in week 9. The length is normalized by the initial number of parent spores. Significance level $p < 0.05$ determined by Tukey test. **C)** Development of network area over 9 weeks. The shaded region indicates the range of standard deviation. Significance level $p < 0.05$ determined by Tukey test. **D)** Formation of new spores over 9 weeks. The shaded region indicates the range of standard deviation. Labels indicate statistical difference at $p < 0.05$ determined by Tukey test. (For interpretation of the references to color in this figure legend, the reader is referred to the Web version of this article.)

$p < 0.0001$, Table 1). In myristic acid conditions, A5 covered a larger area (1131 ± 174 mm^2) than in control conditions (287 ± 148 mm^2, $p < 0.001$, Fig. 2C). Similarly, C2 covered a larger area in myristic acid conditions (1096 ± 183 mm^2) than in control conditions (431 ± 198 mm^2, $p < 0.001$, Fig. 2C).

In the myristic acid treatment, we found that both strains reached a maximum network area of approximately 1000 mm^2 in week 4, after which the area plateaued. This growth plateau was reached despite crystallized myristic acid still clearly visible in the media (Fig. 1). Strain C2 formed denser networks in myristic acid conditions (1.19 ± 0.52 mm/mm^2) than in control conditions (0.29 ± 0.23 mm/mm^2, $p = 0.006$). Strain A5 showed a similar trend of denser networks in myristic acid (0.75 ± 0.24 mm/mm^2) than in control conditions (0.27 ± 0.25 mm/mm^2), however, this difference was not significant ($p = 0.13$). C2 networks produced 36-fold more new spores in myristic acid conditions (135 ± 40.6) compared to control conditions (6.2 ± 6.2, $p < 0.001$, Fig. 2D–Table 1). In contrast, strain A5 produced a small number of spores in myristic acid conditions (6.8 ± 2.3) compared to no spores in control conditions (0 ± 0, $p = 0.003$, Fig. 2D).

Our data were robust to standardization. To account for variation of the initial parent spore numbers, we standardized the network length and area per parent spore. The observed significant effect of treatment was consistent for both maximum network length ($F = 108.3$, $p < 0.001$, Fig. 2B–Table 1), and network area ($F = 38.8$, $p < 0.001$, Table 1).

Table 1
Summary of measured variables of the network experiment for strain A5 and C2 in control (0 mM) and myristic acid (0.5 mM) conditions. Length, area, and density values represent the mean ± standard deviation of the maximum recorded measurement. New spores represent the mean ± standard deviation counted number of new spores in week 9.

	A5		C2	
	0 mM	0.5 mM	0 mM	0.5 mM
Total length (mm)	50.4 ± 14.7	865 ± 381	98.9 ± 47.1	1276 ± 548
Length/parent spore (mm)	4.03 ± 1.18	58.9 ± 24.3	7.01 ± 3.77	90.8 ± 36.4
Network area (mm^2)	287 ± 148	1131 ± 174	431 ± 198	1096 ± 183
Area/parent spore (mm^2)	20.0 ± 7.64	77.9 ± 19.5	32.8 ± 21.7	78.0 ± 8.77
Network density (mm/mm^2)	0.27 ± 0.25	0.75 ± 0.24	0.29 ± 0.23	1.19 ± 0.52
New spores	0 ± 0	6.8 ± 2.3	3.75 ± 4.5	135.3 ± 40.6

3.2. *Effect of external carbon on intracellular flows in time*

We recorded cytoplasmic flow speeds (Suppl. Video 1) at different locations in hyphal networks twice per week to cover a growth period over 2 months. Bidirectional flows were observed in all networks regardless of the strain and treatment.

As hypothesized, we found that the addition of myristic acid led to faster cytoplasmic flow speeds. However, against our expectations, these fast flows occurred mainly early in the experiment and their frequency decreased over time. The factors strain, treatment, timepoint, and the interaction between treatment and timepoint had a significant effect on the flow velocity (strain: $\chi^2 = 7.09$, $p = 0.0078$; treatment: $\chi^2 = 4.99$, $p = 0.025$; timepoint: $\chi^2 = 22.97$, $p = 0.00013$; treatment:timepoint: $\chi^2 = 21.85$, $p = 0.00021$). Pairwise comparisons showed that by the second week cytoplasmic flows were significantly faster in the presence of myristic acid compared to the controls for both strains (Tukey $p < 0.05$) (Fig. 3A). In terms of flow speeds, this translated to an approximately 50% increase in speeds for A5 from 1.57 μm/s in control [95% Confidence Interval: 1.33-1.84] to 2.34 μm/s in myristic acid

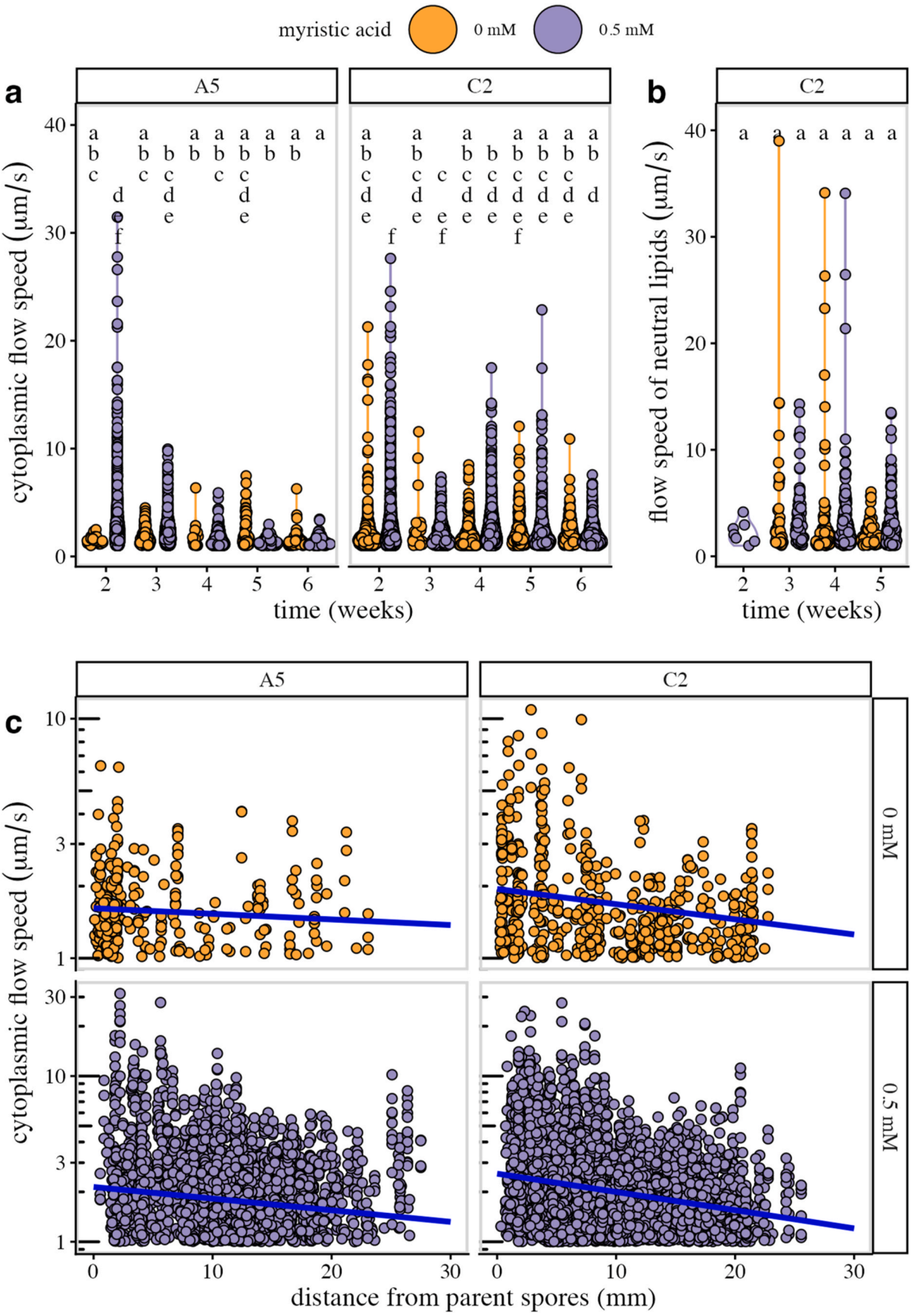

(caption on next page)

Fig. 3. Cytoplasm flow speeds of *R. irregularis* strains A5 and C2 in control (orange) and 0.5 mM myristic acid (purple) conditions. **A)** Brightfield imaging: violin plot of change in flow speed dynamics of A5 and C2 over 6 weeks. Each colored point within the violins represents one flow observation. Different letters indicate statistical significance at $p < 0.05$ according to Tukey post hoc test. **B)** Fluorescence imaging: change in flow speed dynamics of neutral lipids in strain C2 over 5 weeks. Each colored point within the violins represents one flow observation. Neutral lipids were stained with Nile red prior to imaging. Different letters indicate statistical significance at $p < 0.05$ according to Tukey post hoc test. **C)** Flow speed as a function over distance from the parent spores. Each colored point represents one flow observation. Blue lines show the predicted change in flow speed by the linear mixed-effects model. (For interpretation of the references to color in this figure legend, the reader is referred to the Web version of this article.)

conditions [CI: 2.03-2.70]. In C2, speeds increased by 50% from 1.83 μm/s [CI: 1.58-2.12] in control to 2.74 μm/s [CI: 2.39-3.13] in myristic acid conditions (Table 2). In terms of change over time, from week 2 to week 6, cytoplasmic flow speeds in the myristic acid treatment decreased for both strains (Tukey, $p < 0.05$). In week 6, they did not differ from the control treatment anymore (Tukey, $p > 0.05$) – estimated mean velocities were 1.40 μm/s [CI: 1.21-1.62] for A5 and 1.64 μm/s [CI: 1.43-1.89] for C2.

We expected an overall increase in flow speed with myristic acid addition, but instead observed an increase in frequency of relatively infrequent fast flow events. We therefore quantified these speed bursts. We found flow speeds >5 μm/s occurred 669 times, >10 μm/s occurred 116 times, >15 μm/s occurred 32 times, and >30 μm/s only one time (6.9%, 1.2%, 0.5%, and 0.01% of all observations, respectively). Of the 669 observations >5 μm/s, 55% (370 observations) occurred in week 2 and mostly originated from A5 and C2 in myristic acid conditions (179 and 175 observations, respectively). We observed flows >10 μm/s and >15 μm/s in A5 only in the myristic acid conditions in week 2 (37 and 12 times, respectively). The fastest flow measured in this experiment occurred in strain A5 in the myristic acid conditions in week 2. In strain C2, we observed flows >10 and > 15 μm/s in the myristic acid as well as in the control conditions. In myristic acid conditions, however, flows >10 and > 15 μm/s occurred more often (70 and 16 times) than in control conditions (9 and 4 times).

We hypothesized that an increased availability of myristic acid would likewise result in an increased flow speed of lipids more generally within the hyphae. We therefore tested whether the external application of the myristic acid affected the observed mean flow velocity of neutral lipids (i.e., triacylglycerol, a storage lipid that can package various fatty acids including myristic acid) in the strain C2 across time. However, we observed that neither treatment nor the timepoint had an effect on the flow speeds of neutral lipids (all $p > 0.05$, Fig. 3B,Table 2, Suppl. Video 2). The mean flow speed was 3.1 μm/s in control and 3.3 μm/s in myristic acid conditions, suggesting that flow speeds of lipids do not increase regardless of increased carbon availability. To confirm that this finding was not an artifact of the smaller sample size of the fluorescence dataset, we randomly subsampled (without replacement) from the brightfield sample pool to match the sample size of the smaller fluorescence sample pool and repeated the statistical analyses. This was repeated 100 times. The overall pattern of significance for these reduced brightfield datasets stayed comparable to the whole data set (data not shown), indicating that the null effect in the fluorescence dataset relative to the brightfield dataset was not merely a consequence of a smaller sample size in the former.

Table 2
Summary of model outputs of the cytoplasm flow experiment for strain A5 and C2 in control (0 mM) and myristic acid (0.5 mM) conditions. All values represent the model outputs and are the mean speed and mean speed range between the replicates.

week	A5		C2		C2 (Nile red)	
	0 mM	0.5 mM	0 mM	0.5 mM	0 mM	0.5 mM
2	1.57 [1.33 - 1.84] μm/s	2.34 [2.03 - 2.70] μm/s	1.83 [1.58 - 2.12] μm/s	2.74 [2.39 – 3.13] μm/s	NA	2.03 [0.69 - 5.97] μm/s
3	1.58 [1.35 - 1.84] μm/s	1.93 [1.69 - 2.21] μm/s	1.84 [1.57 - 2.16] μm/s	2.26 [2.00 - 2.56] μm/s	2.28 [1.31 - 3.98] μm/s	3.06 [1.64 - 5.72] μm/s
4	1.41 [1.19 - 1.68] μm/s	1.70 [1.48 - 1.94] μm/s	1.65 [1.41 - 1.93] μm/s	1.99 [1.76 – 2.25] μm/s	2.30 [1.39 - 3.80] μm/s	2.26 [1.36 - 3.74] μm/s
5	1.72 [1.48 - 1.99] μm/s	1.50 [1.31 - 1.72] μm/s	2.01 [1.75 - 2.29] μm/s	1.76 [155 – 1.98] μm/s	1.92 [1.07 - 3.47] μm/s	2.35 [1.25 - 4.42] μm/s
6	1.49 [1.25 - 1.77] μm/s	1.40 [1.21 - 1.62] μm/s	1.74 [1.47 - 2.07] μm/s	1.64 [1.43 – 1.89] μm/s	NA	NA

3.3. Effect of external carbon on intracellular flows in space

Given that hyphal growth tended to be denser and more interconnected around parental spores, we asked whether flow speeds were different near spores. We tested the hypothesis that flow speeds would be faster closer to the spore, asking whether strain identity, treatment, time and/or distance to the network origin affected the mean flow velocity. We found that treatment, distance, and the interaction between strain and distance, treatment and distance, and strain, treatment and distance had a significant effect on the flow speed (treatment: $\chi^2 = 10.7$, $p = 0.001$; distance: $\chi^2 = 382.7$, $p < 0.0001$; strain:distance: $\chi^2 = 18.5$, $p < 0.0001$; treatment:distance: $\chi^2 = 12.9$, $p = 0.0003$; strain:treatment:distance: $\chi^2 = 4.4$, $p = 0.04$). We found that fast flows (i.e., maximum flow speeds) occurred more often in closer proximity to the point of origin of the network and estimated flow speeds decreased with increasing distance from the parent spores (Fig. 3C). Namely, for every additional 5 mm distance from the spore, the mean flow speed decreased by an estimated 2.7 % (± SE: 1.1 – 4.2 %).

3.4. Network longevity

Lastly, to determine whether activity of asymbiotic cultures could be maintained for longer periods of time when supplied with myristic acid, we grew 32 networks for 13 to 15 months and screened for cytoplasmic flows. We found cytoplasmic movement in all observed plates regardless of strain and treatment, however, not all these flows were bidirectional (Suppl. Video 3). We hypothesized that unidirectional flows could potentially result from external forces such as air pressure acting on the cytoplasm. We assume that only bidirectional flows would represent cytoplasmic activity. Therefore, we screened the networks for clear bidirectional cytoplasmic flows (Suppl. Video 4). We found that 69% of the networks showed bidirectional, active cytoplasmic flows close to the parent spores regardless of the strain and treatment. In control conditions, 57% of A5 and 67% of C2 plates still showed cytoplasmic activity. In myristic acid conditions, 50% of A5 and 100% of C2 plates were still active around the parent spores. In contrast, outer hyphae had formed septa and were inactive (Suppl. Video 5).

4. Discussion

We used myristic acid as an external carbon and energy source to examine the growth and nutrient flow in AM fungal hyphae that are not connected to a host plant. Our new imaging platform allowed us to document both hyphal growth and cytoplasmic flows. We found that bidirectional flows are an inherent fungal trait not driven by the host

and that hyphal networks can remain active for over one year without host plant interactions. Furthermore, we observed an increase of fast cytoplasmic flow speeds in the presence of myristic acid, but these decreased over time. We found cytoplasmic flow speeds were fastest close to the parent spore and decreased with increasing distance. We found no effect of myristic acid on the flow speed of neutral lipids. Lastly, we found that hyphal networks grew larger, denser, and produced more daughter spores when myristic acid was supplied as an external carbon source.

4.1. Bidirectional flows are present even without host plant interaction

We found that bidirectional cytoplasm flows occur in AM hyphae even when they are not connected to a host, despite the lack of resource trade and a clear source-sink direction (Bago et al., 2002; Oyarte Galvez et al., 2025). The way in which this bidirectionality is maintained remains an open question. One possibility is that built-up, regulated differences in turgor drive the flow in one direction. Bidirectionality could then be achieved by active transport of cellular components in the opposite direction by for example molecular motors (Egan et al., 2012). Studies in the filamentous, septate fungus *Neurospora crassa* and the aseptate oomycete *Achlya bisexualis* have shown that differences in turgor create a pressure gradient in the cytoplasm that facilitates mass flow (Abadeh and Lew, 2013; Lew, 2005; Muralidhar et al., 2016). In *N. crassa*, mass flow is unidirectional at around 2 μm/s (Abadeh and Lew, 2013) and *A. bisexualis* displays bidirectional cytoplasmic flow at a range between 1.6 and 2 μm/s (Muralidhar et al., 2016). As is the case for AM fungi, the identity and exact details of the physiological mechanisms that maintain these bidirectional flows remains an open question. It has been suggested that the tubular vacuole system in AM fungal hyphae that is associated with cytoplasmic flows (Cargill et al., 2025; K. Saito et al., 2004; Uetake et al., 2002) may play a key role in the bidirectionality of flows. Tubular vacuoles have been suggested as means of intracellular long-distance transportation (Cole et al., 1998). In germ tubes and extraradical symbiotic hyphae of *Gigaspora margarita*, bidirectional flows have been reported to occur simultaneously to tubular vacuoles (Uetake et al., 2002). Furthermore, lipid bodies and acidic vesicles have been shown to move bidirectionally alongside this tubular vacuole system of germ tubes (K. Saito et al., 2004). From a functional point of view, the ability to generate bidirectional flows beyond the germination stage may well be essential even for AM fungi growing asymbiotically. Simultaneously to moving carbon and other cellular building blocks to growing tips, they need to be able to move cellular components through their networks, such as nuclei and mitochondria, as well as allocate resources such as lipids to spores for reproduction (Bago et al., 2002; Giovannetti et al., 2000).

4.2. Cytoplasmic activity up to one year after germination

We were surprised that our networks still showed cytoplasmic activity after one year in the absence of a host regardless of the presence or absence of myristic acid. Previously, fungi-only mediated processes could only be studied in the germination stage roughly up to 35 days post germination (Giovannetti et al., 2000, 2010; Kokkoris et al., 2019). By adding myristic acid to the culturing media, the time frame for fungi-only experiments could potentially be extended beyond this mark. Specifically, we found that in 32 surveyed plates, 69% still had cytoplasmic activity concentrated around the parent spores. Strikingly, in the myristic acid conditions only 50% of A5 plates were still active, whereas 100% of C2 plates were still active suggesting that myristic acid could be affecting fitness dynamics. Our findings align with past work that has shown that germinated spores retract their cytoplasm and retain detectable metabolic activity close to the parent spore for up to six months if they do not intercept a host (Logi et al., 1998). The time frame of this present study doubles the previously reported record, although it remains to be investigated whether the spores are still infective at this stage.

The question of ecological importance of these findings remains unanswered. Myristate is a compound in root exudates (S. Li et al., 2017; Pomilio et al., 2000; Xing et al., 2024) and bacterial byproduct (Hildebrandt et al., 2006) in soil environments. From our understanding, there are no studies yet investigating exact mechanisms of AM fungal uptake of myristate (Rillig et al., 2020). For example, future approaches could focus on whether myristate in the soil can be utilized by AM fungi to survive extreme situations where a host is abruptly absent (e.g., due to drought).

4.3. Fast flows occur early and slow down over time

Cytoplasmic flow speeds in AM fungal germlings have been investigated and quantified for decades (Giovannetti et al., 1999, 2000). We recently reported the first systematic quantification of cytoplasmic flow speeds across time and space by measuring over 100,000 flow trajectories in symbiotic AM fungal networks connected to plant roots (Oyarte Galvez et al., 2025). Yet whether and how the behavior of cytoplasmic flows would differ in asymbiotically growing networks with access to a suitable carbon source remained an open question. We hypothesized that similar flow dynamics would be found across symbiotic and asymbiotic networks growing on myristic acid for two reasons: first, myristic acid provides a carbon source for the generation of ATP which could be powering membrane-bound ion pumps and thus potentially driving flows through creating an osmotic gradient. Second, due to increased complexity (i.e., longer, larger, and more interconnected networks) that are formed in the presence of myristic acid, we expected faster flow speeds to occur more frequently than in hyphae in control conditions lacking myristic acid.

We found that asymbiotic flows in the presence of myristic acid averaged speeds of 2.5 μm/s, with faster flows above 5 μm/s as rare events (~1% of all recorded flows) (Fig. 3A). Our data agree with previous findings of cytoplasmic flows in AM fungi occurring in a similar range from 2.5 μm/s up to 5 μm/s in hyphae of germlings (Giovannetti et al., 2000; Hammer et al., 2024; Uetake et al., 2002) and 1.8 μm/s in hyphal fusion bridges between germlings (Giovannetti et al., 1999). Average cytoplasmic flow velocity in symbiotic networks increases over time to around 5 μm/s, with occasional bursts of high speeds of 50 up to 120 μm/s (Oyarte Galvez et al., 2025). The events of fast flow bursts in this present study did not reach these reported speeds. The fast flows were present only in the first few weeks. After week 3, speeds remained very slow, on average 1.5 μm/s which is a similar velocity as reported for hyphal fusion bridges between germlings (Giovannetti et al., 1999). This may be an indication that the fungus relies on other essential nutrients other than carbon that were not sufficiently provided in the media.

We further found that flow speeds were fastest closest to the spores and decreased toward hyphal tips. In symbiotic networks, a similar pattern was observed: flow speed increases linearly with distance from the hyphal tip. For every 10 mm from the hyphal tip, speed increased by 2-fold, with fastest speeds near the roots (Oyarte Galvez et al., 2025). Previous work has found flows towards the hyphal tip to be faster than towards the root (Hammer et al., 2024; Oyarte Galvez et al., 2025). This was hypothesized to reflect spatiotemporal transport requirements and nutrient demands of the fungal network. It must be emphasized that interpretation of the data in our study requires caution as the experimental setup prevents the distinction between flows towards the hyphal tips and flows towards parental spores. This caution must be extended to the interpretation of the spatial component of the recorded flows in the aging network. Due to the increased branching of the network and difficulty in reliable segmentation, the distance between the video coordinates and the network origin (i.e., the parent spore cluster) was determined by a straight line. Therefore, the distance is a proxy rather than the true hyphal length between these points (Suppl. Fig. 2a). However, if future methodology were applied to differentiate the flow directions and measure true distance from the parental spore, this would

provide insight into whether our asymbiotic AM fungi performs similarly to germ tubes and symbiotic AM fungi.

4.4. Flow speed of neutral lipids is unaffected by external myristic acid

We found that flow speeds of neutral lipids remained unaffected and averaged at around 3 μm/s (Fig. 3B). This flow speed is similar to reported lipid movement in extraradical symbiotic hyphae (Bago et al., 2002). By tagging the carbon with Nile red, we tested how speeds of transported carbon changed over time. If lipid transport was driven by mechanical or osmotic pressure gradients along the hyphae, we expected that an increased carbon availability within the network might result in increased speeds of neutral lipids flows. That flow speeds of neutral lipids were unaffected suggests that the lipid transport might be linked to cytoskeletal features (Cargill et al., 2025). Previous studies have closely associated the intracellular transport of lipids to the tubular vacuole system (K. Saito et al., 2004), but another possible mode of transport may be for example molecular motors that operate at limited speeds (C.-B. Li and Toyabe, 2020). However, more research is required to investigate this matter.

4.5. AM fungi maintain a robust growth strategy

Our data confirm that AM fungi can construct complex networks in the absence of a host when myristic acid is present. Previous work had established that myristic acid or myristate can be used as both carbon and energy source by the fungus to support hyphal growth and reproduction (i.e., spore formation) (Sugiura et al., 2020; Tanaka et al., 2022). With our imaging platform, we could precisely follow the construction of these networks for nine weeks (Figs. 1 and 2).

First, we confirmed previous findings that myristic acid functions as an effective external carbon source by showing that myristic acid networks grow on average ~10-fold longer and 3-times denser compared to controls that lacked a carbon source. This agrees with recent research that found that the saturation density of AM fungal networks is under fungal control, specifically that network density (mm/mm^2) does not change regardless of whether a host root is present if myristic acid is supplied (Oyarte Galvez et al., 2025). Our work therefore provides additional evidence for the hypothesis that given a certain amount of carbon, AM fungi employ a specific and autonomous growth strategy (Bisot et al., 2026).

The network growth in our experiments was much slower than the reported growth of symbiotic AM fungi (Oyarte Galvez et al., 2025). In symbiotic growth conditions, *R. irregularis* strains A5 grew roughly 2000 times longer and C2 grew 30 times longer by day 5 than in our asymbiotic experiments (Suppl. Fig. 3). However, due to differences in experimental setup (i.e., plate size and shape) and time frame, these experiments cannot be directly compared and these differences in growth must be interpreted with caution. For example, imaging in the asymbiotic experiments started as soon as spores germinated. Whereas imaging in symbiotic plates began roughly four weeks delayed since fungi first had to germinate, colonize roots, and cross over into a fungal-only arena.

However, we did find that the total area explored by the fungus reached a plateau in both our fungal strains in asymbiotic conditions (Fig. 2C). While there was still crystallized myristic acid in the medium visible by eye, it is hard to rule out whether growth stopped due to carbon limitation. One explanation for this plateau is that fungal growth was limited by essential nutrients other than carbon (e.g., amino acids or peptones as organic nitrogen sources). In previous myristic acid and myristate studies, the media included organic nitrogen (Sugiura et al., 2020; Tanaka et al., 2022). To keep conditions similar to our previous experiments quantifying speeds across symbiotic networks (Oyarte Galvez et al., 2025), the media in the present study contained only contained inorganic nitrogen.

5. Conclusions

Our experiments demonstrate that AM fungi grown on myristic acid as a carbon source still display bidirectional cytoplasmic flows even when they are not connected to a host plant. This challenges our understanding of AM fungal autonomy, by suggesting that cytoplasmic flows can be decoupled from host roots. Our results pose three further questions. First, what is the abundance of alternate carbon sources such as myristic acid and myristate in soil environments? Second, do these alternate carbon sources make a significant contribution to fungal network survival in nature? Third, what are the mechanisms that enable these bidirectional flows? Answers to these questions will advance our knowledge of AM fungal physiology which is important for expanding our comprehension of AM fungi in the ecological context.

CRediT authorship contribution statement

Malin Klein: Conceptualization, Data curation, Formal analysis, Investigation, Validation, Visualization, Writing – original draft, Writing – review & editing. **Loreto Oyarte Gálvez:** Conceptualization, Data curation, Investigation, Methodology, Writing – review & editing. **Daniel van der Lugt:** Investigation, Writing – review & editing. **Corentin Bisot:** Data curation, Methodology, Writing – review & editing. **Simon van Staalduine:** Data curation, Methodology, Writing – review & editing. **Stuart A. West:** Writing – review & editing. **Vasilis Kokkoris:** Funding acquisition, Writing – review & editing. **Lemeng Dong:** Writing – review & editing. **Harro Bouwmeester:** Funding acquisition, Writing – review & editing. **Thomas S. Shimizu:** Resources, Writing – review & editing. **James T. Weedon:** Formal analysis, Writing – review & editing. **E. Toby Kiers:** Conceptualization, Funding acquisition, Writing – review & editing.

Declaration of competing interest

The authors declare that they have no known competing financial interests or personal relationships that could have appeared to influence the work reported in this paper.

Acknowledgements

We thank Hannah Ruppert for her contributions to the pilot experiment that preceded this research. We acknowledge support from the Schmidt Family Foundation, NWO-VICI (202.012), NWO- MICROP (024.004.014), NWO-SPINOZA, HFSP (RGP 0029), ERC (Nuclear Mix, 101076062), and ERC (834164).

Appendix A. Supplementary data

Supplementary data to this article can be found online at https://doi.org/10.1016/j.funbio.2026.101775.

Data availability

All data are available upon request.

References

Abadeh, A., Lew, R.R., 2013. Mass flow and velocity profiles in Neurospora hyphae: partial plug flow dominates intra-hyphal transport. Microbiology (United Kingdom) 159 (PART11), 2386–2394. https://doi.org/10.1099/MIC.0.071191-0/CITE/REFWORKS.

Bago, B., Pfeffer, P.E., Shachar-Hill, Y., 2000. Carbon metabolism and transport in arbuscular mycorrhizas. Plant Physiol. 124 (3), 949–958. https://doi.org/10.1104/pp.124.3.949. https://academic.oup.com/plphys/article/124/3/949/6097492. (Accessed 1 November 2000).

Bago, B., Pfeffer, P.E., Zipfel, W., Lammers, P., Shachar-Hill, Y., 2002a. Tracking metabolism and imaging transport in arbuscular mycorrhizal fungi. Metabolism and

transport in AM fungi. Plant Soil 244 (1), 189–197. https://doi.org/10.1023/A:1020212328955.
Bago, B., Zipfel, W., Williams, R.M., Jun, J., Arreola, R., Lammers, P.J., Pfeffer, P.E., Shachar-Hill, Y., 2002b. Translocation and utilization of fungal storage lipid in the arbuscular mycorrhizal symbiosis. Plant Physiology 128 (1), 108–124. https://doi.org/10.1104/pp.010466.
Bates, D., Mächler, M., Bolker, B., Walker, S., 2015. Fitting linear mixed-effects models using lme4. J. Stat. Software 67 (1), 1–48. https://doi.org/10.18637/jss.v067.i01.
Bisot, C., Galvez, L.O., Kahane, F., van Son, M., Turcu, B., Broekman, R., Lin, K.-K., Bontenbal, P., Winter, M.K., Kokkoris, V., West, S.A., Godin, C., Kiers, E.T., Shimizu, T.S., 2026. Carbon–phosphorus exchange rate constrains density–speed trade-off in arbuscular mycorrhizal fungal growth. Proc. Natl. Acad. Sci. 123 (6), e2512182123. https://doi.org/10.1073/pnas.2512182123.
Brundrett, M.C., Tedersoo, L., 2018. Evolutionary history of mycorrhizal symbioses and global host plant diversity. New Phytol. 220 (4), 1108–1115. https://doi.org/10.1111/nph.14976. https://nph.onlinelibrary.wiley.com/doi/10.1111/nph.14976. (Accessed 22 January 2018).
Cargill, R.I.M., Shimizu, T.S., Kiers, E.T., Kokkoris, V., 2025. Cellular anatomy of arbuscular mycorrhizal fungi. Curr. Biol. 35 (11), R545–R562. https://doi.org/10.1016/j.cub.2025.03.053.
Chen, H., Xiong, T., Guan, B., Huang, J., Zhao, D., Chen, Y., Liang, H., Li, Y., Wu, J., Ye, S., Li, T., Shu, W., Li, J., Wang, Y., 2025. Tap into non-symbiotic carbon? Exogenous myristate fuels the growth of symbiotic arbuscular mycorrhizal fungi but disrupts their carbon-phosphorus exchange with host plants. bioRxiv, 591230. https://doi.org/10.1101/2024.04.26.591230, 2024.04.26.
Cole, L., Orlovich, D.A., Ashford, A.E., 1998. Structure, function, and motility of vacuoles in filamentous fungi. Fungal Genet. Biol. 24 (1), 86–100. https://doi.org/10.1006/fgbi.1998.1051.
Egan, M.J., McClintock, M.A., Reck-Peterson, S.L., 2012. Microtubule-based transport in filamentous fungi. Curr. Opin. Microbiol. 15 (6), 637–645. https://doi.org/10.1016/j.mib.2012.10.003.
Řezáčová, V., Czakó, A., Stehlík, M., Mayerová, M., Šimon, T., et al., 2021. Organic fertilization improves soil aggregation through increases in abundance of eubacteria and products of arbuscular mycorrhizal fungi. Sci. Rep. 11 (1), 12548. https://doi.org/10.1038/s41598-021-91653-x. https://www.nature.com/articles/s41598-021-91653-x. (Accessed 15 June 2021).
Gashgari, R., Selim, S., Abdel-Mawgoud, M., Warrad, M., Habeeb, T.H., et al., 2020. Arbuscular mycorrhizae induce a global metabolic change and improve the nutritional and health benefits of pennyroyal and parsley. Acta Physiol. Plant. 42 (6), 102. https://doi.org/10.1007/s11738-020-03091-3. https://link.springer.com/10.1007/s11738-020-03091-3. (Accessed 24 May 2020).
Giovannetti, M., Avio, L., Sbrana, C., 2010. Fungal spore germination and pre-symbiotic mycelial growth – physiological and genetic aspects. In: Koltai, H., Kapulnik, Y. (Eds.), Arbuscular Mycorrhizas: Physiology and Function. Springer, Netherlands, pp. 3–32. https://doi.org/10.1007/978-90-481-9489-6_1.
Giovannetti, M., Azzolini, D., Citernesi, A.S., 1999. Anastomosis formation and nuclear and protoplasmic exchange in arbuscular mycorrhizal Fungi. Appl. Environ. Microbiol. 65 (Number 12).
Giovannetti, M., Sbrana, C., Logi, C., 2000. Microchambers and video-enhanced light microscopy for monitoring cellular events in living hyphae of arbuscular mycorrhizal fungi. Plant Soil 226 (2), 153–159. https://doi.org/10.1023/A:1026415419193.
Gómez-Leyva, J.F., Segura-Castruita, M.A., Hernández-Cuevas, L.V., Íñiguez-Rivas, M., 2023. Arbuscular mycorrhizal fungi associated with maize (Zea mays L.) in the formation and stability of aggregates in two types of soil. Microorganisms 11 (11), 2615. https://doi.org/10.3390/microorganisms11112615. https://www.mdpi.com/2076-2607/11/11/2615. (Accessed 24 October 2023).
Hammer, E.C., Arellano-Caicedo, C., Mafla-Endara, P.M., Kiers, E.T., Shimizu, T., Ohlsson, P., Aleklett, K., 2024. Hyphal exploration strategies and habitat modification of an arbuscular mycorrhizal fungus in microengineered soil chips. Fungal Ecol. 67, 101302. https://doi.org/10.1016/j.funeco.2023.101302.
Hawkins, H., Cargill, R.I.M., Van Nuland, M.E., Hagen, S.C., Field, K.J., et al., 2023. Mycorrhizal mycelium as a global carbon pool. Curr. Biol. 33 (11), R560–R573. https://doi.org/10.1016/j.cub.2023.02.027. https://linkinghub.elsevier.com/retrieve/pii/S0960982223001677.
Hildebrandt, U., Ouziad, F., Marner, F.-J., Bothe, H., 2006. The bacterium Paenibacillus validus stimulates growth of the arbuscular mycorrhizal fungus Glomus intraradices up to the formation of fertile spores. FEMS (Fed. Eur. Microbiol. Soc.) Microbiol. Lett. 254 (2), 258–267. https://doi.org/10.1111/j.1574-6968.2005.00027.x.
Jiang, Y., Wang, W., Xie, Q., Liu, N., Liu, L., et al., 2017. Plants transfer lipids to sustain colonization by mutualistic mycorrhizal and parasitic fungi. Science 356 (6343), 1172–1175. https://doi.org/10.1126/science.aam9970. https://www.science.org/doi/10.1126/science.aam9970.
Kakouridis, A., Hagen, J.A., Kan, M.P., Mambelli, S., Feldman, L.J., et al., 2022. Routes to roots: direct evidence of water transport by arbuscular mycorrhizal fungi to host plants. New Phytol. 236 (1), 210–221. https://doi.org/10.1111/nph.18281. https://nph.onlinelibrary.wiley.com/doi/10.1111/nph.18281.
Kikuchi, Y., Hijikata, N., Ohtomo, R., Handa, Y., Kawaguchi, M., et al., 2016. Aquaporin-mediated long-distance polyphosphate translocation directed towards the host in arbuscular mycorrhizal symbiosis: application of virus-induced gene silencing. New Phytol. 211 (4), 1202–1208. https://doi.org/10.1111/nph.14016. https://nph.onlinelibrary.wiley.com/doi/10.1111/nph.14016. (Accessed 3 May 2016).
Knegt, Bram, Jansa, Jan, Franken, Oscar, Engelmoer, Daniel J.P., Werner, Gijsbert D.A., et al., 2016. Host plant quality mediates competition between arbuscular mycorrhizal fungi. Fungal Ecol. 20, 233–240. https://doi.org/10.1016/j.funeco.2014.09.011. https://linkinghub.elsevier.com/retrieve/pii/S1754504814001354.
Kohlmeier, M., 2015. Chapter 5 - fatty acids. In: Kohlmeier, M. (Ed.), Nutrient Metabolism, second ed. Academic Press, pp. 111–186. https://doi.org/10.1016/B978-0-12-387784-0.00005-5.
Kokkoris, V., Miles, T., Hart, M.M., 2019. The role of in vitro cultivation on asymbiotic trait variation in a single species of arbuscular mycorrhizal fungus. Fungal Biol. 123 (4), 307–317. https://doi.org/10.1016/j.funbio.2019.01.005.
T. W. Kuyper, X. Wang, M. N. Muchane, The Interplay Between Roots and Arbuscular Mycorrhizal Fungi Influencing Water and Nutrient Acquisition and Use Efficiency, The Root Systems in Sustainable Agricultural Intensification, 29, 4, 2021, 2021, 193, 220, 10.1002/9781119525417.ch7, 9781119525400, https://onlinelibrary.wiley.com/doi/10.1002/9781119525417.ch7, Wiley.
Lenth, R.V., Bolke, B., Buerkner, P., Giné-Vázquez, I., Herve, M., Jung, M., Love, J., Miguez, F., Riebl, H., Singmann, H., 2023. Emmeans: Estimated Marginal Means, Aka Least-Squares Means (R Package Version 1.8.5.). https://CRAN.R-project.org/package=emmeans.
Lew, R.R., 2005. Mass flow and pressure-driven hyphal extension in Neurospora crassa. Microbiology 151 (8), 2685–2692. https://doi.org/10.1099/MIC.0.27947-0/CITE/REFWORKS.
Li, S., Xu, C., Wang, J., Guo, B., Yang, L., Chen, J., Ding, W., 2017. Cinnamic, myristic and fumaric acids in tobacco root exudates induce the infection of plants by Ralstonia solanacearum. Plant Soil 412 (1), 381–395. https://doi.org/10.1007/s11104-016-3060-5.
Li, C.-B., Toyabe, S., 2020. Efficiencies of molecular motors: a comprehensible overview. Biophys. Rev. 12 (2), 419–423. https://doi.org/10.1007/s12551-020-00672-x.
Liu, X., Feng, Z., Zhang, W., Yao, Q., Zhu, H., 2023. Exogenous myristate promotes the colonization of arbuscular mycorrhizal fungi in tomato. Front. Plant Sci. 14, 2023. https://www.frontiersin.org/journals/plant-science/articles/10.3389/fpls.2023.1250684.
Logi, C., Sbrana, C., Giovannetti, M., 1998. Cellular events involved in survival of individual arbuscular Mycorrhizal symbionts growing in the absence of the host. Appl. Environ. Microbiol. 64 (9), 3473–3479. https://doi.org/10.1128/AEM.64.9.3473-3479.1998.
Luginbuehl, L.H., Menard, G.N., Kurup, S., Van Erp, H., Radhakrishnan, G.V., et al., 2017. Fatty acids in arbuscular mycorrhizal fungi are synthesized by the host plant. Science 356 (6343), 1175–1178. https://doi.org/10.1126/science.aan0081. https://www.science.org/doi/10.1126/science.aan0081.
Mangeol, P., Prevo, B., Peterman, E.J.G., 2016. KymographClear and KymographDirect: two tools for the automated quantitative analysis of molecular and cellular dynamics using kymographs. Mol. Biol. Cell 27 (12), 1948–1957. https://doi.org/10.1091/mbc.e15-06-0404.
Šmilauer, P., Košnar, J., Kotilínek, M., Pecháčková, S., Šmilauerová, M., 2021. Host age and surrounding vegetation affect the community and colonization rates of arbuscular mycorrhizal fungi in a temperate grassland. New Phytol. 232 (1), 290–302. https://doi.org/10.1111/nph.17550. https://nph.onlinelibrary.wiley.com/doi/10.1111/nph.17550. (Accessed 12 July 2021).
Šmilauer, P., Košnar, J., Kotilínek, M., Šmilauerová, M., 2019. Contrasting effects of host identity, plant community, and local species pool on the composition and colonization levels of arbuscular mycorrhizal fungal community in a temperate grassland. New Phytol. 225 (1), 461–473. https://doi.org/10.1111/nph.16112. https://nph.onlinelibrary.wiley.com/doi/10.1111/nph.16112. (Accessed 18 September 2019).
Muralidhar, A., Swadel, E., Spiekerman, M., Suei, S., Fraser, M., Ingerfeld, M., Tayagui, A.B., Garrill, A., 2016. A pressure gradient facilitates mass flow in the oomycete Achlya bisexualis. Microbiology 162 (2), 206–213. https://doi.org/10.1099/mic.0.000216.
Oyarte Galvez, L., Bisot, C., Bourrianne, P., Cargill, R., Klein, M., van Son, M., van Krugten, J., Caldas, V., Clerc, T., Lin, K.-K., Kahane, F., van Staalduine, S., Stewart, J. D., Terry, V., Turcu, B., van Otterdijk, S., Babu, A., Kamp, M., Seynen, M., et al., 2025. A travelling-wave strategy for plant–fungal trade. Nature. https://doi.org/10.1038/s41586-025-08614-x.
Pomilio, A.B., Leicach, S.R., Grass, M.Y., Ghersa, C.M., Santoro, M., Vitale, A.A., 2000. Constituents of the root exudate of Avena fatua grown under far-infrared-enriched light. Phytochem. Anal. 11 (5), 304–308. https://doi.org/10.1002/1099-1565(200009/10)11:5<304::AID-PCA531>3.0.CO;2-G.
R Core Team, 2022. R: a Language and Environment for Statistical Computing. R Foundation for Statistical Computing. https://www.R-project.org/.
Rillig, M.C., Aguilar-Trigueros, C.A., Anderson, I.C., Antonovics, J., Ballhausen, M.-B., Bergmann, J., Bielcik, M., Chaudhary, V.B., Deveautour, C., Grünfeld, L., Hempel, S., Lakovic, M., Lammel, D.R., Lehmann, A., Lehmann, J., Leifheit, E.F., Liang, Y., Li, E., Lozano, Y.M., et al., 2020. Myristate and the ecology of AM fungi: significance, opportunities, applications and challenges. New Phytol. 227 (6), 1610–1614. https://doi.org/10.1111/nph.16527.
Saito, K., Kuga-Uetake, Y., Saito, M., 2004. Acidic vesicles in living hyphae of an arbuscular mycorrhizal fungus, Gigaspora margarita. Plant Soil 261 (1), 231–237. https://doi.org/10.1023/B:PLSO.0000035574.54040.c5.
Saito, M., Endo, K., Kobayashi, K., Watanabe, M., Ikeuchi, M., Murakami, A., Murata, N., Wada, H., 2018. High myristic acid content in the cyanobacterium Cyanothece sp. PCC 8801 results from substrate specificity of lysophosphatidic acid acyltransferase. Biochim. Biophys. Acta Mol. Cell Biol. Lipids 1863 (9), 939–947. https://doi.org/10.1016/j.bbalip.2018.05.011.
Schindelin, J., Arganda-Carreras, I., Frise, E., Kaynig, V., Longair, M., Pietzsch, T., Preibisch, S., Rueden, C., Saalfeld, S., Schmid, B., Tinevez, J.-Y., White, D.J., Hartenstein, V., Eliceiri, K., Tomancak, P., Cardona, A., 2012. Fiji: an open-source platform for biological-image analysis. Nat. Methods 9 (7), 676–682. https://doi.org/10.1038/nmeth.2019.

Schubert, A., Allara, P., Morte, A., 2003. Cleavage of sucrose in roots of soybean (Glycine max) colonized by an arbuscular mycorrhizal fungus. New Phytol. 161 (2), 495–501. https://doi.org/10.1046/j.1469-8137.2003.00965.x. https://nph.onlinelibrary.wiley.com/doi/10.1046/j.1469-8137.2003.00965.x. (Accessed 23 December 2003).

Sonnenburg, E.D., Gordon, J.I., 2013. Protein N-Myristoylation. In: Lennarz, W.J., Lane, M.D. (Eds.), Encyclopedia of Biological Chemistry, second ed. Academic Press, pp. 641–644. https://doi.org/10.1016/B978-0-12-378630-2.00021-9.

Stock, S.C., Koester, M., Boy, J., Godoy, R., Nájera, F., et al., 2021. Plant carbon investment in fine roots and arbuscular mycorrhizal fungi: A cross-biome study on nutrient acquisition strategies. Sci. Total Environ. 781, 146748. https://doi.org/10.1016/j.scitotenv.2021.146748. https://linkinghub.elsevier.com/retrieve/pii/S0048969721018167.

Sugiura, Y., Akiyama, R., Tanaka, S., Yano, K., Kameoka, H., Marui, S., Saito, M., Kawaguchi, M., Akiyama, K., Saito, K., 2020. Myristate can be used as a carbon and energy source for the asymbiotic growth of arbuscular mycorrhizal fungi. Proc. Natl. Acad. Sci. 117 (41), 25779–25788. https://doi.org/10.1073/pnas.2006948117.

Tanaka, S., Hashimoto, K., Kobayashi, Y., Yano, K., Maeda, T., Kameoka, H., Ezawa, T., Saito, K., Akiyama, K., Kawaguchi, M., 2022. Asymbiotic mass production of the arbuscular mycorrhizal fungus Rhizophagus clarus. Commun. Biol. 5 (1). https://doi.org/10.1038/s42003-021-02967-5.

Tang, B., Man, J., Lehmann, A., Rillig, M.C., 2023. Arbuscular mycorrhizal fungi benefit plants in response to major global change factors. Ecol. Lett. 26 (12), 2087–2097. https://doi.org/10.1111/ele.14320. https://onlinelibrary.wiley.com/doi/10.1111/ele.14320. (Accessed 4 October 2023).

Torrecillas, E., Alguacil, M.M., Roldán, A., 2012. Host preferences of arbuscular mycorrhizal fungi colonizing annual herbaceous plant species in semiarid mediterranean prairies. Appl. Environ. Microbiol. 78 (17), 6180–6186. https://doi.org/10.1128/aem.01287-12. https://journals.asm.org/doi/10.1128/AEM.01287-12.

Trépanier, M., Bécard, G., Moutoglis, P., Willemot, C., Gagné, S., et al., 2005. Dependence of arbuscular-mycorrhizal fungi on their plant host for palmitic acid synthesis. Appl. Environ. Microbiol. 71 (9), 5341–5347. https://doi.org/10.1128/aem.71.9.5341-5347.2005. https://journals.asm.org/doi/10.1128/AEM.71.9.5341-5347.2005.

Uetake, Y., Kojima, T., Ezawa, T., Saito, M., 2002. Extensive tubular vacuole system in an arbuscular mycorrhizal fungus, Gigaspora margarita. New Phytol. 154 (3), 761–768. https://doi.org/10.1046/j.1469-8137.2002.00425.x.

Wewer, V., Brands, M., Dörmann, P., 2014. Fatty acid synthesis and lipid metabolism in the obligate biotrophic fungus Rhizophagus irregularis during mycorrhization of Lotus japonicus. Plant J. 79 (3), 398–412. https://doi.org/10.1111/tpj.12566. https://onlinelibrary.wiley.com/doi/10.1111/tpj.12566. (Accessed 2 July 2014).

Whiteside, M.D., Werner, G.D.A., Caldas, V.E.A., van't Padje, A., Dupin, S.E., et al., 2019. Mycorrhizal fungi respond to resource inequality by moving phosphorus from rich to poor patches across networks. Curr. Biol. 29 (12), 2043–2050.e8. https://doi.org/10.1016/j.cub.2019.04.061. https://linkinghub.elsevier.com/retrieve/pii/S0960982219304907.

Xing, Z., Zhang, Z., Zhao, Y., Biere, A., Liu, S., Shi, Y., Ding, J., 2024. Foliar herbivory-enhanced mycorrhization is associated with increased levels of lipids in root and root exudates. J. Ecol. 112 (4), 701–716. https://doi.org/10.1111/1365-2745.14272.